PHYSICAL REVIEW D **90,** 054011 (2014)

Higgs-boson production through gluon fusion at NNLO QCD with parton showers

Stefan Höche,[1] Ye Li,[1] and Stefan Prestel[2]

[1]*SLAC National Accelerator Laboratory, Menlo Park, California 94025, USA*
[2]*Deutsches Elektronen-Synchrotron, DESY, 22603 Hamburg, Germany*

(Received 14 July 2014; published 11 September 2014)

We discuss how the UN^{2}LOPS scheme for matching next-to-next-to-leading order (NNLO) calculations to parton showers can be applied to processes with large higher-order perturbative QCD corrections. We focus on Higgs-boson production through gluon fusion as an example. We also present an NNLO fixed-order event generator for this reaction.

DOI: 10.1103/PhysRevD.90.054011 PACS numbers: 12.38.Bx, 12.38.Cy, 14.80.Bn

I. INTRODUCTION

The high precision of experimental measurements at the Large Hadron Collider (LHC) requires equally precise theoretical calculations for the Standard Model processes of interest, such as Higgs-boson production [1]. Experimental analyses often impose intricate kinematical cuts on the final-state phase space, thus calling for fully differential predictions of the cross section. At the same time the resummation of large logarithmic corrections is important, especially in order to describe QCD radiative corrections to the hard process.

These requirements have inspired many new techniques to simulate the structure of hadron collider events with unprecedented accuracy [2]. Among them are the pioneering matching methods MC@NLO [3] and POWHEG [4], which allowed, for the first time, to combine next-to-leading order (NLO) QCD calculations with parton showers by means of a modified subtraction scheme. Even higher precision is needed for Higgs physics, as the dominant production mode through gluon fusion suffers from large perturbative corrections. Next-to-next-to leading order (NNLO) accurate fixed-order predictions [5–7] are routinely employed, NNLO accurate predictions for Higgs plus jet production have been obtained [8] and N^{3}LO accurate results are actively pursued [9]. Mixed QCD and electroweak two-loop corrections have been estimated assuming complete factorization [10] and later evaluated in an effective theory approach [11]. Resummed predictions have been made at NNLO + NNLL [12,13] and at N^{3}LL [14]. Jet vetoed cross sections, particularly relevant for Higgs-boson decay channels involving W bosons have been in the focus of interest recently [15]. The matching of NNLO fixed-order results to parton showers using the MINLO method was presented in [16].

Making the most precise fixed-order predictions available in the framework of general purpose event generators is a challenging task. Three different proposals exist for matching NNLO calculations to parton showers [16–18], but only two of them were implemented so far [16,17,19,20]. The aim of this publication is to discuss one of them, the UN^{2}LOPS matching method, for Higgs boson production at hadron colliders. We also present an independent, fully differential NNLO fixed-order calculation of Higgs-boson production using the q_T-cutoff technique.

This article is organized as follows: Section II reviews the UN^{2}LOPS matching method. Section III discusses the implementation of the NNLO calculation. Alterations of the UN^{2}LOPS proposal [19], needed for the matching in Higgs production, are introduced in Sec. IV. Section V presents our results and Sec. VI gives an outlook.

II. UN^{2}LOPS MATCHING

To set the stage, we recall the refined UN^{2}LOPS method [21] introduced in [19]. We assume MC@NLO matched predictions [3], for Higgs-boson plus zero and one jets, which are to be merged. Any infrared safe observable O is computed in these simulations as

$$\langle O\rangle_n = \int \mathrm{d}\Phi_n \tilde{\mathrm{B}}_n(\Phi_n)\bar{\mathcal{F}}_n(t(\Phi_n),O) + \int \mathrm{d}\Phi_{n+1}\mathrm{H}_n(\Phi_{n+1})\mathcal{F}_{n+1}(t(\Phi_{n+1}),O), \quad (1)$$

where $\mathrm{d}\Phi_n$ denotes the differential n-particle phase-space element, including a convolution with the parton distribution functions (PDFs). We use the following notation for the NLO-weighted Born cross section, $\tilde{\mathrm{B}}$, and the hard remainder function, H:

$$\tilde{\mathrm{B}}_n(\Phi_n) = \mathrm{B}_n(\Phi_n) + \tilde{\mathrm{V}}_n(\Phi_n) + \mathrm{I}_n(\Phi_n) + \int \mathrm{d}\hat{\Phi}_1[\mathrm{S}_n(\Phi_n,\hat{\Phi}_1)\Theta(t_n(\Phi_n) - t_{n+1}(\hat{\Phi}_1)) - \mathrm{D}_n(\Phi_n,\hat{\Phi}_1)]$$
$$\mathrm{H}_n(\Phi_{n+1}) = \mathrm{B}_{n+1}(\Phi_{n+1}) - \mathrm{D}_n(\Phi_{n+1})\Theta(t_n(\Phi_n) - t_{n+1}(\Phi_{n+1})). \quad (2)$$

The functions B_n, $\tilde{\mathrm{V}}_n$ and S_n represent the Born, virtual and real subtraction contribution to the n-jet NLO calculation, while I_n stands for the integrated subtraction terms [22]. $\mathrm{d}\hat{\Phi}_1$ represents the one-emission differential phase-space element, which factorizes as $\mathrm{d}\hat{\Phi}_1 = \mathrm{d}t\mathrm{d}z\mathrm{d}\phi/(2\pi)J(t,z)$, with $J(t,z)$ being a Jacobian factor.

The generating functional of the parton shower, $\mathcal{F}_n(t,O)$, is defined using the parton-shower evolution kernels, K_n.

$$\mathcal{F}_n(t,O) = \Pi_n(t_c,t)O(\Phi_n) + \int_{t_c}^{t} \mathrm{d}\hat{\Phi}_1 \mathrm{K}_n(\hat{\Phi}_1)\Pi_n(\hat{t},t)\mathcal{F}_{n+1}(\hat{t},O). \quad (3)$$

The no-branching probability, Π_n, follows from the unitarity condition $\mathcal{F}_n(t,1) = 1$. We use the abbreviations $t_n = t(\Phi_n)$ and $\hat{t} = t(\hat{\Phi}_1)$ to denote the evolution scales for the n-particle process and the additional emission generated in the integration over $\mathrm{d}\hat{\Phi}_1$. Similarly, we define a generating functional for the MC@NLO.

$$\bar{\mathcal{F}}_n(t,O) = \tilde{\Pi}_n(t_c,t)O(\Phi_n) + \int_{t_c}^{t} \mathrm{d}\hat{\Phi}_1 \frac{\mathrm{D}_n(\Phi_n,\hat{\Phi}_1)}{\mathrm{B}_n(\Phi_n)} \tilde{\Pi}_n(\hat{t},t)\mathcal{F}_{n+1}(\hat{t},O). \quad (4)$$

We restrict real corrections in the zero-jet MC@NLO to transverse momenta $q_T < q_{T,\mathrm{cut}}$ (denoted by $\mathrm{H}_1^{q_{T,\mathrm{cut}}}$), and we choose $q_{T,\mathrm{cut}}$ such that it falls below the parton-shower cutoff, t_c. At the same time the one-jet calculation is regularized by requiring Higgs-boson transverse momenta larger than $q_{T,\mathrm{cut}}$. This implies that resolved real corrections are generated solely by the one-jet MC@NLO. In order to reproduce the logarithmic structure of the parton-shower prediction, the emission terms must be weighted by the all-order resummed virtual and unresolved corrections [23], which are obtained in the form of a no-branching probability computed by the parton shower. At the same time, coupling renormalization and some higher-logarithmic corrections [24,25] are accounted for by reweighting with the appropriate ratio of coupling constants. This reweighting introduces $\mathcal{O}(\alpha_s)$ terms that impair the NLO accuracy. They are subtracted by the first-order expansion of the weight factor, and by the first-order expansion of the no-branching probability, $\Pi_0^{(1)}(t_1,\mu_Q^2)$ [19].

$$\begin{aligned}\langle O\rangle_1 = \int_{q_{T,\mathrm{cut}}} \mathrm{d}\Phi_1 [&\mathrm{B}_1(\Phi_1)\Pi_0(t_1,\mu_Q^2)(w_1(\Phi_1) + w_1^{(1)}(\Phi_1) \\ &+ \Pi_0^{(1)}(t_1,\mu_Q^2)) + \tilde{\mathrm{B}}_1^{\mathrm{R}}(\Phi_1)\Pi_0(t_1,\mu_Q^2)]\bar{\mathcal{F}}_1(t_1,O) \\ &+ \int_{q_{T,\mathrm{cut}}} \mathrm{d}\Phi_2 [\mathrm{H}_1^{\mathrm{R}}(\Phi_1)\Pi_0(t_1,\mu_Q^2) + \mathrm{H}_1^{\mathrm{E}}(\Phi_1)]\mathcal{F}_2(t_2,O).\end{aligned} \quad (5)$$

We have defined $\tilde{\mathrm{B}}^{\mathrm{R}} = \tilde{\mathrm{B}} - \mathrm{B}$ and the regular and exceptional parts of the real corrections, H^{R} and H^{E}. They correspond to two-parton configurations with and without a parton-shower equivalent, respectively [19]. μ_Q^2 defines the resummation scale. The weight factor w_1 is given as

$$w_1(\Phi_1) = \frac{\alpha_s(bt_1)}{\alpha_s(\mu_R^2)} \frac{f_a(x_a,t_1)}{f_a(x_a,\mu_F^2)} \frac{f_{a'}(x_{a'},\mu_F^2)}{f_{a'}(x_{a'},t_1)}$$
$$\text{where } \beta_0 \ln\frac{1}{b} = \left(\frac{67}{18} - \frac{\pi^2}{6}\right) C_A - \frac{10}{9} T_R n_f, \quad (6)$$

and where $f_a(x_a)$ and $f_{a'}(x_{a'})$ denote the PDFs associated with the external and intermediate parton (in the sense of a parton-shower history). The scale factor b includes effects of the two-loop cusp anomalous dimension in the parton shower [25,26].

The restricted zero-jet calculation and the one-jet MC@NLO result above $q_{T,\mathrm{cut}}$ do not overlap. We can thus replace the zero-jet MC@NLO by a full q_T-vetoed NNLO calculation, using the cutoff method [27], and complete the cross section using the one-jet MC@NLO [19]: Each event removed from the one-jet bin by means of the emission probability $1 - \Pi_0(t,\mu_Q^2)$ is added to the zero-jet bin. This unitarization procedure is equivalent to a parton-shower resummation of the jet veto cross section at $q_{T,\mathrm{cut}}$. It gives the UN^{2}LOPS matching formula

$$\begin{aligned}\langle O\rangle^{(\mathrm{UN^2LOPS})} = &\int \mathrm{d}\Phi_0 \bar{\bar{\mathrm{B}}}_0^{q_{T,\mathrm{cut}}}(\Phi_0)O(\Phi_0) + \int_{q_{T,\mathrm{cut}}} \mathrm{d}\Phi_1 [1 - \Pi_0(t_1,\mu_Q^2)(w_1(\Phi_1) + w_1^{(1)}(\Phi_1) + \Pi_0^{(1)}(t_1,\mu_Q^2))]\mathrm{B}_1(\Phi_1)O(\Phi_0) \\ &+ \int_{q_{T,\mathrm{cut}}} \mathrm{d}\Phi_1 \Pi_0(t_1,\mu_Q^2)(w_1(\Phi_1) + w_1^{(1)}(\Phi_1) + \Pi_0^{(1)}(t_1,\mu_Q^2))\mathrm{B}_1(\Phi_1)\bar{\mathcal{F}}_1(t_1,O) \\ &+ \int_{q_{T,\mathrm{cut}}} \mathrm{d}\Phi_1 [1 - \Pi_0(t_1,\mu_Q^2)]\tilde{\mathrm{B}}_1^{\mathrm{R}}(\Phi_1)O(\Phi_0) + \int_{q_{T,\mathrm{cut}}} \mathrm{d}\Phi_1 \Pi_0(t_1,\mu_Q^2)\tilde{\mathrm{B}}_1^{\mathrm{R}}(\Phi_1)\bar{\mathcal{F}}_1(t_1,O) \\ &+ \int_{q_{T,\mathrm{cut}}} \mathrm{d}\Phi_2 [1 - \Pi_0(t_1,\mu_Q^2)]\mathrm{H}_1^{\mathrm{R}}(\Phi_2)O(\Phi_0) + \int_{q_{T,\mathrm{cut}}} \mathrm{d}\Phi_2 \Pi_0(t_1,\mu_Q^2)\mathrm{H}_1^{\mathrm{R}}(\Phi_2)\mathcal{F}_2(t_2,O) \\ &+ \int_{q_{T,\mathrm{cut}}} \mathrm{d}\Phi_2 \mathrm{H}_1^{\mathrm{E}}(\Phi_2)\mathcal{F}_2(t_2,O),\end{aligned} \quad (7)$$

where $\bar{\bar{B}}_0^{q_{T,\mathrm{cut}}}$ represents the q_T-vetoed NNLO cross section, differential in the Born phase space. By construction the inclusive cross section exactly reproduces the NNLO result.

III. THE q_T-VETOED NNLO CALCULATION

In the dominant production mode at hadron colliders, the Higgs boson couples to two gluons via heavy quark loops. The full top and bottom quark mass dependent gluon fusion cross section is known to NLO only [28]. It is more convenient to work in an effective theory (HEFT), where the heavy top quark is integrated out [29]. The gluon fusion process is then described by the effective Lagrangian,

$$\mathcal{L}_{\mathrm{eff}} = -\frac{\alpha_s}{4v}\frac{c_g}{3\pi} H G^a_{\mu\nu} G_a^{\mu\nu}, \tag{8}$$

where v is the Higgs vacuum expectation value, and $c_g = 1 + \mathcal{O}(\alpha_s)$ is the Wilson coefficient. Quark mass effects can be incorporated *a posteriori*. The matching to the Higgs effective theory leads to a factorized form of the hard function. We write it schematically as

$$H(Q^2,\mu^2) = |c_g|^2 = \sum_{n=0}\left(\frac{\alpha_s(\mu^2)}{4\pi}\right)^n h^{(n)}(Q^2,\mu^2). \tag{9}$$

The hard function can be improved by including an additional overall factor of the full top mass dependent leading order (LO) gluon fusion cross section, normalized by the HEFT LO cross section. This is a very good approximation at NNLO [30,31]. The hard function is applied to the NNLO results of effective theory order by order in α_s, i.e. $h^{(2)}$ only multiplies the LO HEFT cross section, $h^{(1)}$ multiplies the NLO HEFT cross section and $h^{(0)}$ multiplies the NNLO HEFT cross section. A similar scheme can be used in the matched calculation. However, we can also multiply the hard function as an overall factor to the HEFT calculation, leading to a second possible matching scheme, which will be discussed in Sec. IV.

The NNLO Higgs production in the Higgs effective theory implemented in Sherpa is based on the q_T subtraction method [6,32]. It separates the two-loop NNLO calculation into a zero-q_T bin, leaving the phase space with finite q_T to the NLO calculation. This matches well with the general structure of UN^{2}LOPS , introduced in Sec. II. The dependence on the q_T cutoff, used to define the zero-q_T bin, cancels between contributions from the two phase-space regions. Given a small enough q_T cutoff, the zero-q_T bin can be mapped onto the Born phase space, as all soft and collinear radiation is integrated over. For Higgs or Drell-Yan processes, where there is no final-state colored particle at Born level, the q_T cut roughly corresponds to the parton-shower cutoff scale. In addition, the zero-q_T bin follows a simple factorization formula, which generates very compact results for $\bar{\bar{B}}_0^{q_{T,\mathrm{cut}}}$ that can easily be implemented numerically. The remainder is computed as Higgs-boson plus one-jet production at NLO, using [33] for the virtual matrix elements and the Catani-Seymour subtraction method for regularizing real radiative corrections [34].

As a consequence of the factorization, the zero-q_T bin contribution can be written as a differential K factor to the Born level cross section

$$\frac{\int_0^{q_{T,\mathrm{cut}}} \mathrm{d}q_T \int_{x_i}^1 \mathrm{d}\xi_i \int_{x_j}^1 \mathrm{d}\xi_j C_{ij\to gg}(q_T, \frac{x_i}{\xi_i}, \frac{x_j}{\xi_j}, \mu) f_i(\xi_i,\mu_F^2) f_j(\xi_j,\mu_F^2)}{f_g(x_i,\mu_F^2) f_g(x_j,\mu_F^2)}, \tag{10}$$

where $C_{ij\to gg}$ is the hard collinear coefficient, and $f_i(x_i,\mu_F^2)$ refers to the PDF. The factorization formula describes the vetoed Higgs NNLO cross section up to power corrections in the cutoff, $q_{T,\mathrm{cut}}$.

The hard collinear coefficient is derived using the framework developed in [13] and using recent two-loop results given in [35]. The results have been verified against those presented in [36]. In the framework of Sherpa, our implementation is fully differential in phase space, which allows us to generate events at the parton level. Additionally, Higgs-boson decays to arbitrary final states can be included.

IV. UN^{2}LOPS IN HIGGS-BOSON PRODUCTION

Higgs-boson production via gluon fusion suffers from large perturbative corrections, both to the inclusive cross section and to the shape of distributions like the transverse momentum of the Higgs boson. This necessitates a careful treatment of higher-order effects in the matching to parton showers. In processes like Drell-Yan lepton pair production—where perturbative corrections to the transverse momentum distribution are small—different matching schemes will lead to similar results in the sense that any possible difference cannot be resolved experimentally. The situation is just the opposite in Higgs-boson production, which was pointed out in several comparisons of NLO matching methods [22,37]. We discuss the problem in this section, and we propose two different strategies to tackle processes with large higher-order corrections.

Equation (7) proposes to subtract the no-branching probabilities, Π_0, only when they multiply the leading-order part, B_1, of the one-jet MC@NLO result. This is a minimal approach. The expansion of the no-branching probabilities in powers of the strong coupling generates terms of $\mathcal{O}(\alpha_s^3)$ when multiplied by $\tilde{B}_1$ or H_1, which is beyond the required NNLO accuracy of UN^{2}LOPS. It is thus acceptable to also subtract these no-branching probabilities. A factorization of the subtractions of w_1 and Π_0 multiplying the B_1 term also only amounts to changing orders beyond the formal accuracy:

$$\Pi_0(t_1,\mu_Q^2)(w_1(\Phi_1)+w_1^{(1)}(\Phi_1)+\Pi_0^{(1)}(t_1,\mu_Q^2)) \to \Pi_0(t_1,\mu_Q^2)(1+\Pi_0^{(1)}(t_1,\mu_Q^2))(w_1(\Phi_1)+w_1^{(1)}(\Phi_1))\mathrm{B}_1(\Phi_1). \quad (11)$$

Finally, evaluating PDFs and α_s in $\Pi_0^{(1)}$ with running scales is legitimate. We will redefine $\Pi_0^{(1)}$ in this way below. After these changes, the revised UN^{2}LOPS matching formula reads

$$\begin{aligned}
\langle O\rangle^{(\mathrm{UN^2LOPS})} = {} & \int \mathrm{d}\Phi_0 \bar{\bar{\mathrm{B}}}_0^{q_{T,\mathrm{cut}}}(\Phi_0)O(\Phi_0) + \int_{q_{T,\mathrm{cut}}} \mathrm{d}\Phi_1[1-\Pi_0(t_1,\mu_Q^2)(1+\Pi_0^{(1)}(t_1,\mu_Q^2))(w_1(\Phi_1)+w_1^{(1)}(\Phi_1))]\mathrm{B}_1(\Phi_1)O(\Phi_0) \\
& + \int_{q_{T,\mathrm{cut}}} \mathrm{d}\Phi_1 \Pi_0(t_1,\mu_Q^2)(1+\Pi_0^{(1)}(t_1,\mu_Q^2))(w_1(\Phi_1)+w_1^{(1)}(\Phi_1))\mathrm{B}_1(\Phi_1)\bar{\mathcal{F}}_1(t_1,O) \\
& + \int_{q_{T,\mathrm{cut}}} \mathrm{d}\Phi_1[1-\Pi_0(t_1,\mu_Q^2)(1+\Pi_0^{(1)}(t_1,\mu_Q^2))]\tilde{\mathrm{B}}_1^{\mathrm{R}}(\Phi_1)O(\Phi_0) \\
& + \int_{q_{T,\mathrm{cut}}} \mathrm{d}\Phi_1 \Pi_0(t_1,\mu_Q^2)(1+\Pi_0^{(1)}(t_1,\mu_Q^2))\tilde{\mathrm{B}}_1^{\mathrm{R}}(\Phi_1)\bar{\mathcal{F}}_1(t_1,O) \\
& + \int_{q_{T,\mathrm{cut}}} \mathrm{d}\Phi_2[1-\Pi_0(t_1,\mu_Q^2)(1+\Pi_0^{(1)}(t_1,\mu_Q^2))]\mathrm{H}_1^{\mathrm{R}}(\Phi_2)O(\Phi_0) \\
& + \int_{q_{T,\mathrm{cut}}} \mathrm{d}\Phi_2 \Pi_0(t_1,\mu_Q^2)(1+\Pi_0^{(1)}(t_1,\mu_Q^2))\mathrm{H}_1^{\mathrm{R}}(\Phi_2)\mathcal{F}_2(t_2,O) + \int_{q_{T,\mathrm{cut}}} \mathrm{d}\Phi_2 \mathrm{H}_1^{\mathrm{E}}(\Phi_2)\mathcal{F}_2(t_2,O). \quad (12)
\end{aligned}$$

This again integrates to the NNLO cross section, while preserving the parton-shower accuracy as well as the one-jet NLO result up to higher orders in α_s. The changes to the one-jet contribution of the UN^{2}LOPS formula may be interpreted as a complete subtraction of $\mathcal{O}(\Gamma)$ contributions from the parton shower, where the branching probability, $\Gamma(t,Q^2)=\mathrm{d}\log\Pi(t,Q^2)/\mathrm{d}t$, is the natural expansion parameter of the resummation. Compared to the procedure described in [19], we obtain the following additional contribution to the one-jet bin:

$$\begin{aligned}
& \int_{q_{T,\mathrm{cut}}} \mathrm{d}\Phi_1 \Pi_0(t_1,\mu_Q^2)\Pi_0^{(1)}(t_1,\mu_Q^2) \\
& \quad \times [\tilde{\mathrm{B}}_1^{\mathrm{R}}(\Phi_1)+\mathrm{B}_1(\Phi_1)(w_1(\Phi_1)-1+w_1^{(1)}(\Phi_1))]\bar{\mathcal{F}}_1(t_1,O) \\
& \quad + \int_{q_{T,\mathrm{cut}}} \mathrm{d}\Phi_2 \Pi_0(t_1,\mu_Q^2)\Pi_0^{(1)}(t_1,\mu_Q^2)\mathrm{H}_1^{\mathrm{R}}(\Phi_2)\mathcal{F}_2(t_2,O).
\end{aligned} \quad (13)$$

These terms are clearly beyond the formal accuracy of the UN^{2}LOPS method. Including them emphasizes the fixed-order result at medium q_T and therefore removes some arbitrariness introduced by the parton-shower resummation. It can thus be expected to be an improvement over the method presented in [19], even though a thorough assessment can only be made after matching to N^{3}LO fixed-order results. The implementation of Eq. (12) in a Monte Carlo event generator is described in Appendix A.

In Eq. (12), $\bar{\bar{\mathrm{B}}}_0^{q_{T,\mathrm{cut}}}$ does not affect exclusive observables. However, the hard function coming from the square of Wilson coefficients of the Higgs effective theory in $\bar{\bar{\mathrm{B}}}_0$ is universal, and it should in fact appear also in differential distributions at higher orders, as it factorizes from real-radiative corrections. It might be beneficial to single out such contributions. We therefore define two variants of the UN^{2}LOPS method, which use the Wilson coefficients to improve the simulation of the one-jet process. This is very similar to the MC@NLO and POWHEG methods, as discussed in [19].

The two possible ways of dealing with the factorized hard function $H(Q^2,\mu^2)=\sum[\alpha_s(\mu^2)/(4\pi)]^n h^{(n)}(Q^2,\mu^2)$ are the following:

(1) "individual" matching
   (a) Terms multiplying $h^{(0)}$ are matched using UN^{2}LOPS
   (b) Terms multiplying $h^{(1)}$ are matched using MC@NLO
   (c) Terms multiplying $h^{(2)}$ are showered
(2) "factorized" matching
   (a) The NNLO result in HEFT, ignoring the Wilson coefficient, is matched using UN^{2}LOPS
   (b) The matched result is multiplied by H in Eq. (9)

Note that the factorized matching increases the cross section by a few percent (see Sec. V). This increase can legitimately be considered as part of the large NNLO theoretical uncertainty in the Higgs-production process.

V. RESULTS

This section presents results using an implementation of the UN^{2}LOPS algorithm in the event generator Sherpa [38]. We use a parton shower [39] based on Catani-Seymour dipole subtraction [34]. NLO virtual corrections

TABLE I. Total cross sections at varying center-of-mass energy for a pp-collider. Uncertainties from scale variations are given as sub-/superscripts. Statistical uncertainties from Monte Carlo integration are quoted in parentheses.

E_{cms}	7 TeV	14 TeV	33 TeV	100 TeV
HNNLO	$13.494(7)^{+1.436}_{-1.382}$ pb	$44.550(16)^{+4.293}_{-3.954}$ pb	$160.84(13)^{+13.29}_{-12.36}$ pb	
SHERPA	$13.515(7)^{+1.433}_{-1.382}$ pb	$44.559(36)^{+4.226}_{-3.929}$ pb	$160.39(17)^{+13.47}_{-11.88}$ pb	$670.1(10)^{+47.9}_{-39.4}$ pb

for the one-jet process [33] are taken from MCFM [40]. Dipole subtraction is performed using Amegic [41] and cross-checked with Comix [42]. We use the MSTW 2008 PDF set [43] and the corresponding definition of the running coupling. We work in the five flavor scheme. Electroweak parameters are given as $G_F = 1.1663787 \times 10^{-5}$ GeV^{-2}, $m_H = 125$ GeV. The results are derived in the limit $m_t \gg m_H$. Predictions for finite m_t will be given elsewhere.

In order to cross-check our implementation we first compare the total cross section to results obtained from HNNLO [6,7]. Table I shows that the predictions agree within the permille-level statistical uncertainty of the Monte Carlo integration. Additionally, we have checked

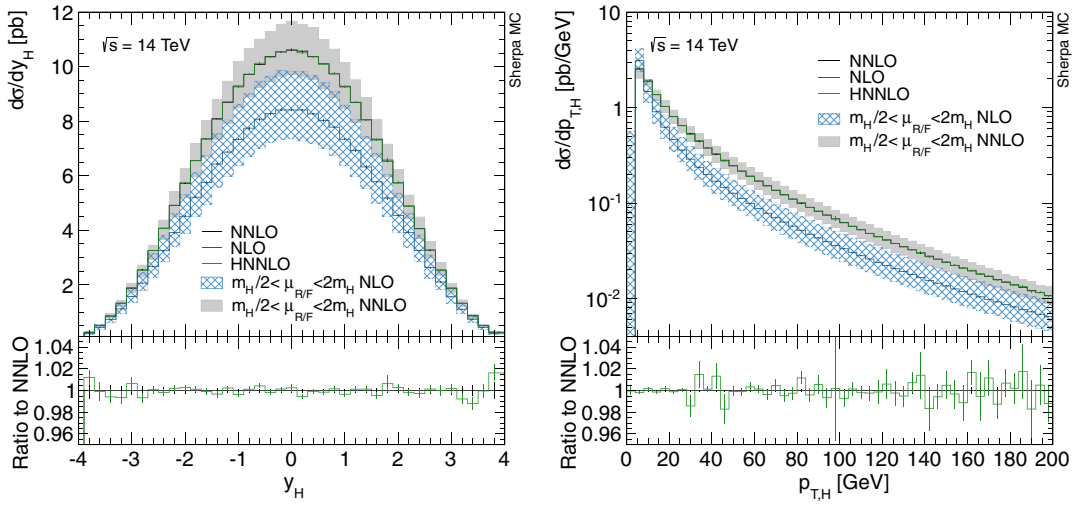

FIG. 1 (color online). Rapidity spectrum (left) and transverse momentum spectrum (right) of the Higgs boson, computed at fixed order and compared between Sherpa and HNNLO .

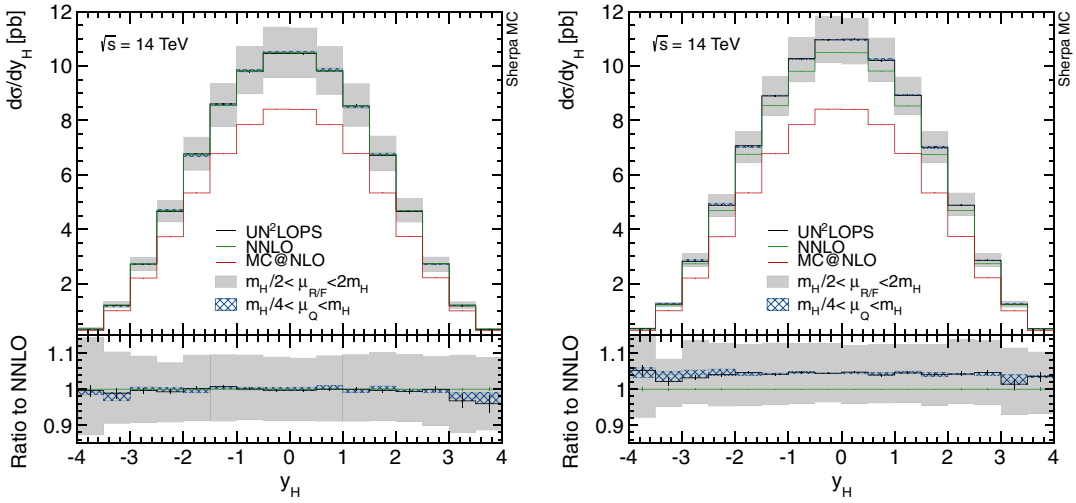

FIG. 2 (color online). Rapidity spectrum of the Higgs boson in individual matching (left) and factorized matching (right). See Sec. IV for details.

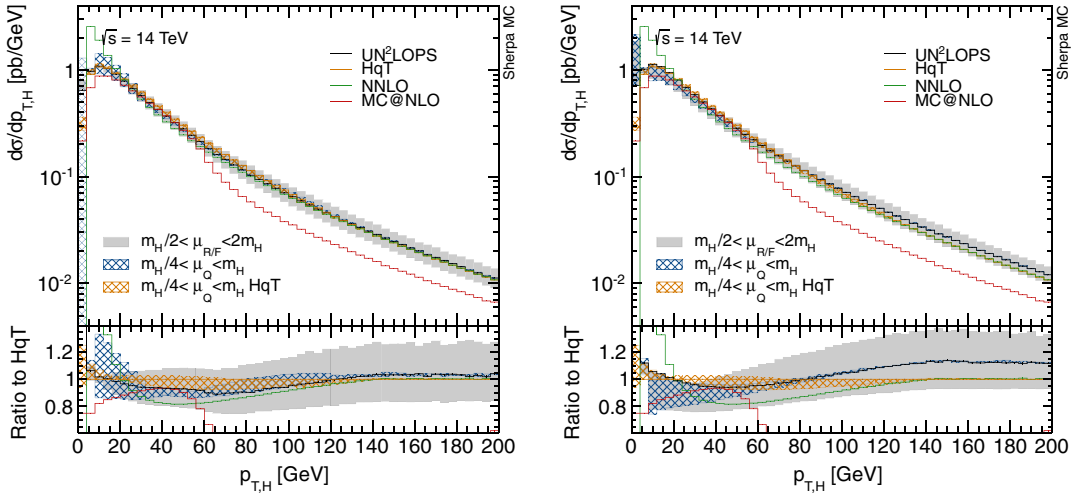

FIG. 3 (color online). Transverse momentum spectrum of the Higgs boson in individual matching (left) and factorized matching (right). See Sec. IV for details.

that our results are identical when varying $q_{T,\mathrm{cut}}$ between 0.1 and 1 GeV. The default value is $q_{T,\mathrm{cut}} = 1$ GeV. Figure 1 shows a comparison of the Higgs rapidity and transverse momentum spectrum between Sherpa and HNNLO. The excellent agreement over a wide range of phase space confirms the correct implementation of the NNLO calculation in Sherpa.

Figure 2 compares fixed-order predictions for the rapidity spectrum of the Higgs boson to matched results from UN^{2}LOPS. Both the individual and factorized matching approach, introduced in Sec. IV, yield perfect agreement for the shape of the distribution, while the factorized matching also slightly increases the cross section (see Sec. IV).

Figure 3 compares the UN^{2}LOPS matched results for the Higgs boson transverse momentum to predictions from HqT [44], which performs an analytic matching of the q_T spectrum at NLO + NNLL accuracy. As expected, the resummation uncertainty in UN^{2}LOPS is larger. Nevertheless, the central predictions agree quite well. This indicates that the impact of possible higher-logarithmic contributions should be small enough to be neglected for the purpose of event generation at the 14 TeV LHC, provided that the central resummation scale is set appropriately. Similar findings were reported for $t\bar{t}$ production in [45].

The zero-q_T bin is clearly problematic. This can be understood as follows: In our calculation the q_T spectrum is described only at NLO + NLL accuracy [25,46]. Therefore it suffers from large scale variations, particularly in the soft and collinear region. Equation (12) implies that an increased veto probability in this region also increases the cross section in the zero-q_T bin. The large variation at zero-q_T should thus be reduced significantly once the parton shower is amended with higher-logarithmic resummation. Note, however, that no such variation is present for inclusive observables like the Higgs-boson rapidity spectrum, Fig. 2.

VI. CONCLUSIONS

We presented the first application of the UN^{2}LOPS matching procedure to Higgs-boson production through gluon fusion. This reaction suffers from large higher-order corrections, and several refinements of the original UN^{2}LOPS approach are suggested to improve the matching. They allow us to obtain phenomenologically useful results despite the low logarithmic accuracy of the parton shower compared to analytic approaches. Our predictions are in fair agreement with higher-logarithmic resummation for a resummation scale of $\mu_Q \sim m_H/2$.

We also provide an independent implementation of a fully differential NNLO calculation of Higgs-boson production at hadron colliders, using the q_T-cutoff method, which allows the production of LHEF files [47] or NTuple files [48] containing NNLO event information at parton level.

Due to the fully exclusive nature of our simulations, it is straightforward to combine them with higher-multiplicity NLO calculations using an extension of the MENLOPS method [49] to NNLO. This can be achieved by separating the generating functionals into a hard and a soft part and using appropriately weighted NLO calculations in the hard jet domain. A similar scheme, which also preserves the total cross section, could be based on the UNLOPS method [21,50]. Such a simulation will improve upon our predictions as soon as the Higgs-boson plus two-jet process is included at NLO. We leave the detailed study of the phenomenological implications to future work.

ACKNOWLEDGMENTS

We thank Marek Schönherr and Thomas Lübbert for discussions and Valentin Hirschi and Gionata Luisoni for careful cross-checks of the virtual corrections to Higgs plus one-jet production. We are indebted to Lance Dixon, Frank

Krauss, Leif Lönnblad and HuaXing Zhu for helpful conversations and comments on the manuscript. This work was supported by the U.S. Department of Energy under Contract No. DE–AC02–76SF00515. We used resources of the National Energy Research Scientific Computing Center, which is supported by the Office of Science of the U.S. Department of Energy under Contract No. DE–AC02–05CH11231.

APPENDIX: UN^{2}LOPS STEP BY STEP

This Appendix provides a step-by-step guide to the UN^{2}LOPS method, which allows us to implement the technique in other processes of interest. We focus on reactions at hadron colliders, the generalization to lepton colliders being a straightforward modification. We assume that a vetoed NNLO cross section, computed along the lines of Sec. III, exists. Any other method to provide this cross section can be used, for example a fully exclusive NNLO calculation restricted to $q_T < q_{T,\mathrm{cut}}$ by means of a q_T veto.

(1) Generate a parton-level event according to $\bar{\bar{\mathrm{B}}}_0^{q_{T,\mathrm{cut}}}$, B_1, $\tilde{\mathrm{B}}_1^{\mathrm{R}}$ or H_1.

(2) If $\bar{\bar{\mathrm{B}}}_0^{q_{T,\mathrm{cut}}}$ is selected, skip the parton-shower step.

(3) If B_1, $\tilde{\mathrm{B}}_1$ of H_1 is selected, apply the clustering algorithm described in [51] to define a parton-shower history. If no history is found on H_1 events, they are classified as exceptional. In this case, simply run the parton shower starting from the two-particle state.

(4) In B_1 events, reweight with w_1 in Eq. (6) and subtract the first-order expansion, $w_1^{(1)}$.

(5) Run a truncated parton shower on the zero-jet configuration as identified by backward clustering in step 3. Skip the first emission [52]. If the parton shower generates a second emission, reduce the one- or two-particle configuration to the zero-particle configuration identified in step 3 and do not apply any further parton shower or MC@NLO. If the parton shower does not generate a second emission, and the event was of $\tilde{\mathrm{B}}_1$ type, perform the MC@NLO starting from the one-particle state. If the event was of $\mathrm{H}_1^{\mathrm{R}}$ type, run the parton shower, starting from the two-particle state.

[1] S. Dittmaier *et al.* (LHC Higgs Cross Section Working Group), Report No. 10.5170/CERN-2011-002, 2011; Report No. 10.5170/CERN-2012-002, 2012; S. Heinemeyer *et al.* (LHC Higgs Cross Section Working Group), Report No. 10.5170/CERN-2013-004, 2013.
[2] A. Buckley *et al.*, Phys. Rep. **504**, 145 (2011).
[3] S. Frixione and B. R. Webber, J. High Energy Phys. 06 (2002) 029.
[4] P. Nason, J. High Energy Phys. 11 (2004) 040; S. Frixione, P. Nason, and C. Oleari, J. High Energy Phys. 11 (2007) 070.
[5] C. Anastasiou and K. Melnikov, Nucl. Phys. **B646**, 220 (2002); R. V. Harlander and W. B. Kilgore, Phys. Rev. Lett. **88**, 201801 (2002); V. Ravindran, J. Smith, and W. L. van Neerven, Nucl. Phys. **B665**, 325 (2003); C. Anastasiou, K. Melnikov, and F. Petriello, Nucl. Phys. **B724**, 197 (2005); V. Ravindran, Nucl. Phys. **B752**, 173 (2006).
[6] S. Catani and M. Grazzini, Phys. Rev. Lett. **98**, 222002 (2007).
[7] M. Grazzini, J. High Energy Phys. 02 (2008) 043; S. Catani and M. Grazzini, *Proc. Sci.*, RADCOR2007 (2007) 046.
[8] R. Boughezal, F. Caola, K. Melnikov, F. Petriello, and M. Schulze, J. High Energy Phys. 06 (2013) 072.
[9] C. Anastasiou, C. Duhr, F. Dulat, F. Herzog, and B. Mistlberger, J. High Energy Phys. 12 (2013) 088; W. B. Kilgore, Phys. Rev. D **89**, 073008 (2014); C. Anastasiou, C. Duhr, F. Dulat, E. Furlan, T. Gehrmann, F. Herzog, and B. Mistlberger, arXiv:1403.4616; R. D. Ball, M. Bonvini, S. Forte, S. Marzani, and G. Ridolfi, Nucl. Phys. **B874**, 746 (2013); Y. Li and H. X. Zhu, J. High Energy Phys. 11 (2013) 080; C. Duhr and T. Gehrmann, Phys. Lett. B **727**, 452 (2013); Y. Li, A. von Manteuffel, R. M. Schabinger, and H. X. Zhu, arXiv:1404.5839; T. Ahmed, M. Mandal, N. Rana, and V. Ravindran, arXiv:1404.6504.
[10] S. Actis, G. Passarino, C. Sturm, and S. Uccirati, Phys. Lett. B **670**, 12 (2008).
[11] C. Anastasiou, R. Boughezal, and F. Petriello, J. High Energy Phys. 04 (2009) 003.
[12] D. de Florian and M. Grazzini, Phys. Lett. B **674**, 291 (2009); D. de Florian, G. Ferrera, M. Grazzini, and D. Tommasini, J. High Energy Phys. 06 (2012) 132.
[13] T. Becher, M. Neubert, and D. Wilhelm, J. High Energy Phys. 05 (2013) 110.
[14] M. Bonvini and S. Marzani, arXiv:1405.3654 [J. High Energy Phys. (to be published)].
[15] A. Banfi, G. P. Salam, and G. Zanderighi, J. High Energy Phys. 06 (2012) 159; A. Banfi, P. F. Monni, G. P. Salam, and G. Zanderighi, Phys. Rev. Lett. **109**, 202001 (2012); I. W. Stewart, F. J. Tackmann, J. R. Walsh, and S. Zuberi, Phys. Rev. D **89**, 054001 (2014); T. Becher and M. Neubert, J. High Energy Phys. 07 (2012) 108; T. Becher, M. Neubert, and L. Rothen, J. High Energy Phys. 10 (2013) 125.
[16] K. Hamilton, P. Nason, C. Oleari, and G. Zanderighi, J. High Energy Phys. 05 (2013) 082; K. Hamilton, P. Nason, E. Re, and G. Zanderighi, J. High Energy Phys. 10 (2013) 222.
[17] N. Lavesson and L. Lönnblad, J. High Energy Phys. 12 (2008) 070.
[18] S. Alioli, C. W. Bauer, C. Berggren, F. J. Tackmann, J. R. Walsh, and S. Zuberi, J. High Energy Phys. 06 (2014) 089.

[19] S. Höche, Y. Li, and S. Prestel, arXiv:1405.3607.
[20] A. Karlberg, E. Re, and G. Zanderighi, arXiv:1407.2940.
[21] L. Lönnblad and S. Prestel, J. High Energy Phys. 03 (2013) 166.
[22] S. Höche, F. Krauss, M. Schönherr, and F. Siegert, J. High Energy Phys. 09 (2012) 049.
[23] D. Amati, A. Bassetto, M. Ciafaloni, G. Marchesini, and G. Veneziano, Nucl. Phys. **B173**, 429 (1980).
[24] Y. L. Dokshitzer, D. Diakonov, and S. Troian, Report No. SLAC-TRANS-0183, 1978; D. Amati, R. Petronzio, and G. Veneziano, Nucl. Phys. **B146**, 29 (1978); R. K. Ellis, H. Georgi, M. Machacek, H. D. Politzer, and G. G. Ross, Phys. Lett. **78B**, 281 (1978); S. B. Libby and G. F. Sterman, Phys. Lett. **78B**, 618 (1978); A. H. Mueller, Phys. Rev. D **18**, 3705 (1978); Y. L. Dokshitzer, D. Diakonov, and S. I. Troian, Phys. Rep. **58**, 269 (1980).
[25] S. Catani, B. R. Webber, and G. Marchesini, Nucl. Phys. **B349**, 635 (1991).
[26] J. Kodaira and L. Trentadue, Phys. Lett. B **123**, 335 (1983); S. Catani and L. Trentadue, Nucl. Phys. **B327**, 323 (1989); S. Catani, E. D'Emilio, and L. Trentadue, Phys. Lett. B **211**, 335 (1988); S. Catani, L. Trentadue, G. Turnock, and B. R. Webber, Nucl. Phys. **B407**, 3 (1993).
[27] J. Gao, C. S. Li, and H. X. Zhu, Phys. Rev. Lett. **110**, 042001 (2013).
[28] D. Graudenz, M. Spira, and P. Zerwas, Phys. Rev. Lett. **70**, 1372 (1993); M. Spira, A. Djouadi, D. Graudenz, and P. Zerwas, Phys. Lett. B **318**, 347 (1993); M. Spira, A. Djouadi, D. Graudenz, and P. M. Zerwas, Nucl. Phys. **B453**, 17 (1995); C. Anastasiou, S. Bucherer, and Z. Kunszt, J. High Energy Phys. 10 (2009) 068.
[29] J. R. Ellis, M. K. Gaillard, and D. V. Nanopoulos, Nucl. Phys. **B106**, 292 (1976); F. Wilczek, Phys. Rev. Lett. **39**, 1304 (1977); M. A. Shifman, A. Vainshtein, M. Voloshin, and V. I. Zakharov, Sov. J. Nucl. Phys. **30**, 711 (1979); J. R. Ellis, M. Gaillard, D. V. Nanopoulos, and C. T. Sachrajda, Phys. Lett. **83B**, 339 (1979).
[30] A. Pak, M. Rogal, and M. Steinhauser, J. High Energy Phys. 02 (2010) 025.
[31] R. V. Harlander and K. J. Ozeren, J. High Energy Phys. 11 (2009) 088; R. V. Harlander, H. Mantler, S. Marzani, and K. J. Ozeren, Eur. Phys. J. C **66**, 359 (2010).
[32] S. Catani, L. Cieri, G. Ferrera, D. de Florian, and M. Grazzini, Phys. Rev. Lett. **103**, 082001 (2009).
[33] V. Ravindran, J. Smith, and W. Van Neerven, Nucl. Phys. **B634**, 247 (2002).
[34] S. Catani and M. H. Seymour, Nucl. Phys. **B485**, 291 (1997).
[35] T. Gehrmann, T. Lübbert, and L. L. Yang, J. High Energy Phys. 06 (2014) 155; *Proc. Sci.*, RADCOR2013 (2014) 011.
[36] S. Catani and M. Grazzini, Eur. Phys. J. C **72**, 2013 (2012).
[37] S. Alioli, P. Nason, C. Oleari, and E. Re, J. High Energy Phys. 04 (2009) 002; P. Nason and B. Webber, Annu. Rev. Nucl. Part. Sci. **62**, 187 (2012).
[38] T. Gleisberg, S. Höche, F. Krauss, A. Schälicke, S. Schumann, and J. Winter, J. High Energy Phys. 02 (2004) 056; T. Gleisberg, S. Höche, F. Krauss, M. Schönherr, S. Schumann, F. Siegert, and J. Winter, J. High Energy Phys. 02 (2009) 007.
[39] S. Schumann and F. Krauss, J. High Energy Phys. 03 (2008) 038; S. Catani, S. Dittmaier, M. H. Seymour, and Z. Trocsanyi, Nucl. Phys. **B627**, 189 (2002).
[40] J. M. Campbell and R. Ellis, Nucl. Phys. B, Proc. Suppl. **205–206**, 10 (2010); J. Campbell, R. K. Ellis, and C. Williams, http://mcfm.fnal.gov.
[41] F. Krauss, R. Kuhn, and G. Soff, J. High Energy Phys. 02 (2002) 044; T. Gleisberg and F. Krauss, Eur. Phys. J. C **53**, 501 (2008).
[42] T. Gleisberg and S. Höche, J. High Energy Phys. 12 (2008) 039.
[43] A. D. Martin, W. J. Stirling, R. S. Thorne, and G. Watt, Eur. Phys. J. C **63**, 189 (2009).
[44] G. Bozzi, S. Catani, D. de Florian, and M. Grazzini, Phys. Lett. B **564**, 65 (2003); Nucl. Phys. **B737**, 73 (2006); D. de Florian, G. Ferrera, M. Grazzini, and D. Tommasini, J. High Energy Phys. 11 (2011) 064.
[45] R. Corke and T. Sjöstrand, Eur. Phys. J. C **69**, 1 (2010).
[46] S. Plätzer and S. Gieseke, J. High Energy Phys. 01 (2011) 024.
[47] J. Alwall *et al.*, Comput. Phys. Commun. **176**, 300 (2007); J. Butterworth, G. Dissertori, S. Dittmaier, D. de Florian, N. Glover *et al.*, arXiv:1405.1067.
[48] R. Brun and F. Rademakers, Nucl. Instrum. Methods Phys. Res., Sect. A **389**, 81 (1997); Z. Bern, L. J. Dixon, F. Febres Cordero, S. Höche, H. Ita, D. A. Kosower, and D. Maître, Comput. Phys. Commun. **185**, 1443 (2014).
[49] K. Hamilton and P. Nason, J. High Energy Phys. 06 (2010) 039; S. Höche, F. Krauss, M. Schönherr, and F. Siegert, J. High Energy Phys. 08 (2011) 123.
[50] S. Plätzer, J. High Energy Phys. 08 (2013) 114.
[51] J. André and T. Sjöstrand, Phys. Rev. D **57**, 5767 (1998).
[52] S. Höche, F. Krauss, M. Schönherr, and F. Siegert, J. High Energy Phys. 04 (2013) 027.